# Surface Degradation and Hydrophobic Recovery of Polyolefins Treated by Air Corona and Nitrogen Atmospheric Pressure Glow Discharge

**Sébastien Guimond,* Michael R. Wertheimer**

*Groupe des Couches Minces (GCM), Department of Engineering Physics, Ecole Polytechnique, Montreal, Quebec, H3C 3A7, Canada*

Received 6 February 2004; accepted 28 June 2004
DOI 10.1002/app.21134
Published online in Wiley InterScience (www.interscience.wiley.com).

**ABSTRACT:** The surface degradation and production of low molecular weight oxidized materials (LMWOM) on biaxially oriented polypropylene (BOPP) and low-density polyethylene (LDPE) films was investigated and compared for two different dielectric barrier discharge (DBD) treatment types, namely air corona and nitrogen atmospheric pressure glow discharge ($N_2$ APGD). Contact angle measurements, X-ray photoelectron spectroscopy (XPS), and atomic force microscopy (AFM) analyses were performed in conjunction with rinsing the treated films in water. It is shown that $N_2$ APGD treatments of both polyolefins result in much less surface degradation, therefore, allowing for a significantly higher degree of functionalization and better wettability. Hydrophobic recovery of the treated films has also been studied by monitoring their surface energy ($\gamma_s$) over a period of time extending up to several months after treatment. Following both surface modification techniques, the treated polyolefin films were both found to undergo hydrophobic recovery; however, for $N_2$ APGD modified surfaces, $\gamma_s$ ceases to decrease after a few days and attains a higher stable value than in the case of air corona treated films. © 2004 Wiley Periodicals, Inc. J Appl Polym Sci 94: 1291–1303, 2004

**Key words:** polyolefins; surfaces; modification; aging; morphology; degradation

## INTRODUCTION

Dielectric barrier discharges (DBD) in air, commonly called air corona, are widely used in industry to improve the wetting and adhesion properties of polymers.[1–4] These discharges are usually generated in the gap between two parallel electrodes, at least one of these being covered with a dielectric layer. The presence of this dielectric barrier prevents the discharge from developing into an electrical arc, thereby assuring quasi-non-equilibrium plasma conditions (so-called cold plasma).[5,6] The polymer films to be treated are moved through the discharge gap, where their surface is exposed to the reactive species of the plasma. This process introduces a variety of oxidized chemical functional groups onto the surface of the polymers, increasing their surface energy ($\gamma_s$) and conveying to them a hydrophilic character.[1,7–10] The main advantage of DBDs over low-pressure plasmas is that they are obtained at atmospheric pressure, thereby obviating the need for costly vacuum systems.

Nevertheless, the incorporation of new functional groups at the surface of polymers by air corona has limitations. For certain applications (for instance, the wetting of polyolefins by water-based inks), it may even be problematic to attain a high enough $\gamma_s$ value. Two major causes of this limitation are treatment-induced surface degradation of polymers (which is known to result in the production of low molecular weight oxidized materials or LMWOM[3]), and so-called hydrophobic recovery of the modified surfaces. These two phenomena have a significant technological impact and are the focus of the present article.

The oxidation of polyolefins by air corona is believed to proceed via a free-radical, chain-reaction mechanism.[9,11] In this process, free radicals created at the polymer surface by hydrogen abstraction can form covalent chemical bonds with reactive species in the gas phase ($O_2$, O, OH, etc). While such reactions result in oxygen incorporation at the surface, some of them also lead to cleavage of C—C bonds in the polymer chains. Thus, as the treatment proceeds, increasingly lighter oligomers are generated at the surface, some light enough to be removed from the surface as gaseous products; eventually, equilibrium is reached between such "etching" reactions and oxygen incorporation. The highly oxidized oligomers formed thereby are frequently called LMWOM and have been observed on polyolefin film surfaces treated with high-

*Correspondence to:* M. R. Wertheimer (michel.wertheimer@courriel.polymtl.ca).
* *Present address:* Fritz-Haber-Institut der Max-Planck-Gesellschaft, Faradayweg 4-6, 14195 Berlin, Germany.

energy dose air corona by numerous authors.[3,7,10,12–15] LMWOM can be removed from the treated surfaces by wiping or rinsing with polar solvents; it thus forms a loosely bonded layer that may be harmful for certain applications requiring good adhesion.[16]

Hydrophobic recovery, also called aging, is a phenomenon that originates from the natural, thermodynamically driven tendency of surfaces to lower their free energy, $\gamma_s$. It is manifested by a gradual decrease of the treated polymer's $\gamma_s$ towards its initial value. Aging is commonly observed for corona-treated polymers, and in some cases, much of the beneficial effect of the treatment is already lost after a few weeks.[7,11,17]

Based on the foregoing considerations, there exists much interest in investigating new treatment types that might help resolve these problems. One possible approach, the use of atmospheric pressure glow discharges (APGD) for the modification of polymer films, has recently been reported by several groups.[18–21] Such discharges can be obtained by using very similar DBD configurations as the ones encountered in conventional corona treatment systems, but they are characterized by quite different physics and chemistry.[6,22–26] In an APGD, the plasma zone expands uniformly over the entire electrode area (the DBD is homogeneous), contrary to air corona, where a multitude of microdischarge channels are distributed more or less randomly over the dielectric-coated electrode (filamentary DBD). In recent years, APGDs have received increasing interest, in both academia and industry. Their underlying science and applications for surface modification, thin-film deposition, and other areas are now being widely investigated. In many cases, the quasi-homogeneous character of the APGD can provide advantages over traditional filamentary DBD; the APGD state is readily achieved in noble gases (Ar, He) and in nitrogen, by using high-voltage excitation frequencies in the multi-kilohertz range.

In a recent communication, we have shown that nitrogen atmospheric pressure glow discharges ($N_2$ APGD) can be used advantageously for the surface modification of biaxially oriented polypropylene (BOPP).[20] In that case, we found that $N_2$ APGD treatment can lead to much higher $\gamma_s$ values ($\gamma_s \sim 57$ mN/m) than air corona treatments ($\gamma_s \sim 40$ mN/m). Massines et al.[19] also compared the modification of polypropylene films by several types of DBD and concluded that $N_2$ APGD can lead to a greater wettability than treatment in air. Nevertheless, few data have been reported so far concerning surface degradation or hydrophobic recovery of $N_2$ APGD treated polymers.

In the present work, we extend our earlier investigations to a second polyolefin, low-density polyethylene (LDPE). For both BOPP and LDPE, surface degradation and the production of LMWOM during $N_2$ APGD and air corona treatments are compared. Contact angle measurements along with X-ray photoelectron spectroscopy (XPS) and atomic force microscopy (AFM) analyses have been carried out, before and after rinsing the treated films with water, results being reported as a function of the energy density (dose) of the treatments. Following this, the hydrophobic recovery of modified BOPP and LDPE surfaces is reported, for both treatment types.

## EXPERIMENTAL

### Polymer characteristics

The availability of well-characterized starting materials is of prime importance when studying hydrophobic recovery and plasma-induced surface degradation of polymers. Indeed, these phenomena can be strongly influenced by certain properties of polymer films, for example, the average molecular weight, the presence of additives, etc.[17,27]

The polypropylene used here is a melt-extruded, isotactic BOPP, graciously provided by the 3M Company. The film is 50 $\mu$m thick; the base resin contains $\sim$ 200 ppm of an inorganic acid scavenger and about 1000 ppm of a high molecular weight hindered phenolic antioxidant. It is characterized by a melting point of 163°C, a weight-average molecular weight of $3.6 \times 10^5$, and a polydispersity index of 4.0.

The second polyolefin studied here is a melt-extruded LDPE film, supplied through the courtesy of the Chevron Phillips Chemical Co. It is 35 $\mu$m thick and contains no additives. The base resin has a weight-average molecular weight of $1.2 \times 10^5$ and a polydispersity index of 5.3.

No oxygen was detected by XPS on the untreated surfaces of either film. By using the method of Owens, Wendt and Kaelble,[28] surface energies ($\gamma_s$) of $27 \pm 1$ and $28 \pm 1$ mN/m were measured for the untreated BOPP and LDPE, respectively.

### DBD treatments

The experimental setup, which has been used for both $N_2$ APGD and corona DBD treatments, is presented schematically in Figure 1. The same system was used in our previous work, and its detailed description can be found elsewhere.[20] It consists of a $29 \times 24$ cm grounded Al plate electrode that can be moved linearly at a precisely controlled speed under a cylindrical, high-voltage (HV) electrode. Both electrodes are covered with a dielectric: the former with a thin (2 mm) glass plate, and the latter with a 0.36-mm plasma-sprayed ceramic coating. The polymer film to be treated was placed on the surface of the thin glass plate covering the flat, grounded electrode, the interelectrode gas gap being fixed at 1 mm throughout the study. The treatment system was housed in a hermetic

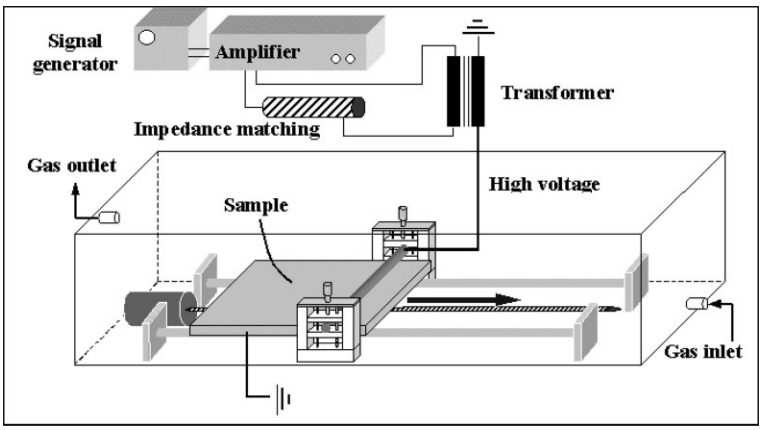


**Figure 1** Schematic view of the DBD experimental treatment setup.

Plexiglas enclosure, which was continuously flushed with a 9-slm flow of the desired treatment gas (dry air for corona and UHP-grade nitrogen for APGD); prior to treatments, the enclosure was purged for 15 min before igniting the discharge. In the case of $N_2$ APGD treatments, the pure $N_2$ flow was directed into a diffuser, enclosing the cylindrical high-voltage electrode (not shown in Fig. 1). This assured a low level of gaseous impurities in the treatment zone, from both the feed gas and the volatile products from the polymer surface. We and others found this to be necessary, because $N_2$ APGD can revert to a filamentary discharge if the impurity concentration exceeds a few hundred ppm.[25,26]

To confirm that the DBD was indeed of the glow type, not filamentary, the photomultiplier signal of light emitted from the gap and the discharge current waveform were monitored on an oscilloscope: in the case of APGD, both are manifested by only a single broad peak per half cycle of the applied voltage. In contrast, a filamentary type of discharge gives rise to many short ($\sim$ 10 ns) pulses of varying amplitudes during each half cycle.[25] For both treatment types, APGD and corona, the energy density, $E_d$, was calculated by using the expression:

$$E_d = \frac{P}{ws}\, n \quad (\mathrm{J/cm^2}) \tag{1}$$

where $P$ is the electrical power dissipated in the gas (in W), $w$ is the width of the discharge zone (24 cm), $n$ is the number of passes of the film through the discharge zone, and $s$ is the effective speed of movement under the electrode (in cm/s). In turn, $s = l/t$, where $l$ is the length of the discharge zone ($\sim$ 1 cm) and $t$ is the residence time. The true rms voltage applied across the gap of flowing gas was typically 3.7 kV. Discharge frequencies, $f$, of 1 and 4 kHz were used for all corona and $N_2$ APGD treatments, respectively; in the case of $N_2$ APGD, we found that results are independent of the discharge frequency, for 1 kHz $\leq f \leq$ 6 kHz (evidently, for constant $E_d$).[20]

### Analytical procedures

As mentioned earlier, surface energy, AFM, and XPS data were obtained for samples as a function of $E_d$, both before and after rinsing: immediately after each treatment, a piece of the treated film was immersed in a bath of deionized water for 1 min and then dried for 1 h in ambient air. Following this, contact angle measurements were made on both the rinsed and the as-treated portions of the sample. XPS and AFM data were acquired within at most 48 h after treatments. Given that Strobel et al.[3] showed that only brief contact with water suffices to remove the LMWOM from the surface of a DBD-treated polyolefin, our 1-min immersion is deemed quite sufficient.

Aging of the modified surfaces was assessed from $\gamma_s$ values of selected samples at various time intervals after their treatment (up to 100 and 200 days for BOPP and LDPE, respectively). Care was taken to use a fresh portion of the sample for each determination. Between measurements, samples were stored in separate Petri dish containers, in a controlled air atmosphere at 50% RH and $T \approx 23$°C. We report here only the aging of as-treated samples.

XPS analyses were performed in a VG ESCALAB 3MkII system, using a nonmonochromatic Mg K$\alpha$ X-ray source (operated at a nominal power of about 220 W). Spectra were acquired normal to the sample surface, and the binding energies were referenced to the carbon (C1s) peak at 285.0 eV, adjustment being made for possible charging effects. Surface energies were determined from measurements of static contact angles with several probe-liquids, according to the method first proposed by Owens, Wendt, and Kaelble.[28] This method allows one to determine the

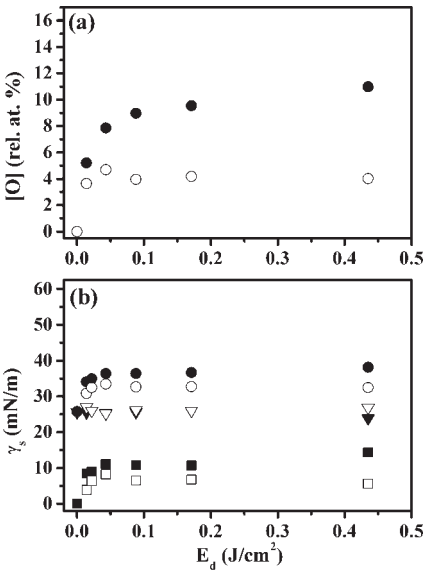


**Figure 2** Effect of water rinsing on air corona-treated BOPP, as a function of the energy dose, $E_d$. (a) Surface concentration of oxygen, [O]. (b) Surface energy, $\gamma_s$, (●), and its polar, $\gamma_s^p$, (■), and dispersive, $\gamma_s^d$, (▼), components. Open symbols pertain to the rinsed samples.

total surface energy ($\gamma_s$), along with its polar ($\gamma_s^p$) and dispersive ($\gamma_s^d$) components. For each liquid (water, glycerol, formamide, ethylene glycol, and tricresyl phosphate), static contact angles of 2-$\mu$L droplets were measured on five different areas of the treated surface, using a Ramé-Hart goniometer (model 100-00). The $\gamma_s$ values presented here have an uncertainty of about ±1 mN/m. AFM measurements were carried out with a Dimension 3100 scanning probe microscope from Digital Instruments, operated in TappingMode®, with etched silicon cantilever probes having a radius of curvature between 5 and 10 nm and a resonant frequency of about 217 kHz. To ascertain the reproducibility of the data, images were acquired on at least four different areas of each sample surface. Parameters like the scan speed, the scanning direction, and the set-point ratio (ratio of the amplitude of the cantilever oscillation at the imaging set-point to the amplitude of its oscillation in free space) were varied so as to exclude possible imaging artifacts. For all images presented in this work, the scan rate was 1 Hz and the set-point ratio was about 0.7.

## RESULTS AND DISCUSSION

### Production of LMWOM: Surface energy and composition

The evolution of $\gamma_s$ as a function of $E_d$ for both water-rinsed and nonrinsed (as-treated) air corona treated BOPP samples is shown in Figure 2(b): the filled symbols correspond to the latter surfaces, the open ones correspond to their rinsed counterparts. The dispersive ($\gamma_s^d$) and polar ($\gamma_s^p$) components of the surface energy ($\gamma_s$) are also shown in this figure, where $\gamma_s = \gamma_s^p + \gamma_s^d$. The corresponding surface oxygen concentrations, [O] (relative atomic %), determined by XPS, are shown in Figure 2(a). (Note that the selected range of $E_d$ values in Figure 2 is representative of those used in industrial applications.[3,4])

From Figure 2(a), it is evident that much of the bound oxygen (LMWOM) is removed from the treated surfaces by rinsing, increasingly so with rising $E_d$, beginning at the threshold value $E_d \sim 0.01$ J/cm$^2$. This energy dose threshold for LMWOM generation agrees quite well with the value reported by Strobel et al. ($E_d \sim 0.05$ J/cm$^2$) in a similar study of the same BOPP.[3] Interestingly, for $E_d > 0.01$ J/cm$^2$, all rinsed samples have nearly identical [O] values ([O] ~ 4%) and surface energies ($\gamma_s \sim 33$ mN/m). All these findings are compatible with the oxidation mechanism comprising both surface functionalization and chain scission reactions:[9,11,29]: for $E_d \leq 0.01$ J/cm$^2$, [O] and $\gamma_s$ increase rapidly due to oxidation of the polymer chains; C—C bond scissions are probably insufficient to generate detectable amounts of water-soluble oligomers. However, for $E_d > 0.01$ J/cm$^2$, chain scissions become more abundant and give rise to the highly oxidized, water-soluble fragments, LMWOM. In the present case, it appears that an equilibrium between oxygen incorporation onto chains and LMWOM generation occurs quite rapidly, which limits the degree of surface functionalization to the observed [O] ~ 4%.

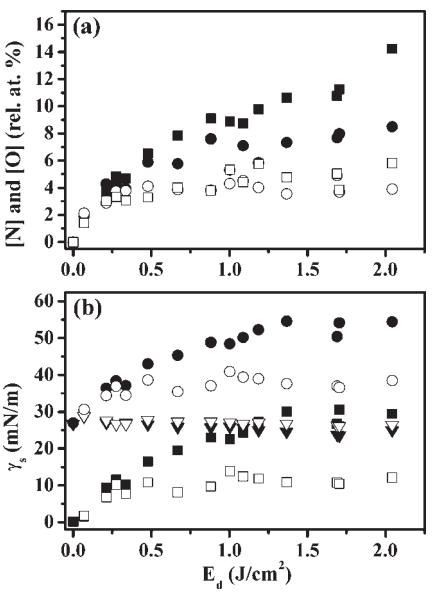


**Figure 3** Effect of water rinsing on $N_2$ APGD treated BOPP, as a function of the energy dose, $E_d$. (a) Surface concentrations of nitrogen, [N], (■), and oxygen, [O] (●). (b) Surface energy, $\gamma_s$, (●), and its polar, $\gamma_s^p$, (■), and dispersive, $\gamma_s^d$, (▼), components. Open symbols pertain to the rinsed samples.

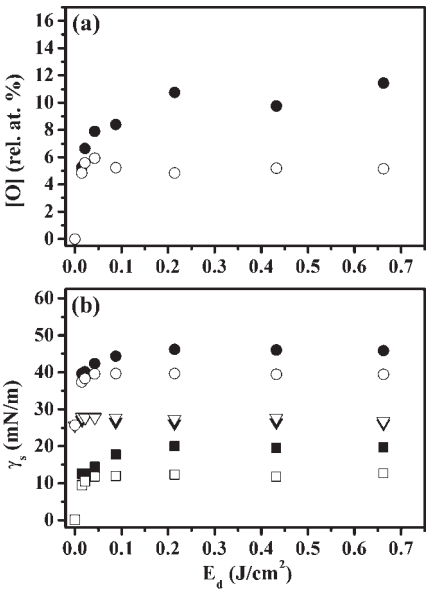


**Figure 4** Effect of water rinsing on air corona treated LDPE, as a function of the energy dose, $E_d$. (a) Surface concentration of oxygen, [O]. (b) Surface energy, $\gamma_s$, (●), and its polar, $\gamma_s^p$, (■), and dispersive, $\gamma_s^p$, (▼), components. Open symbols pertain to the rinsed samples.

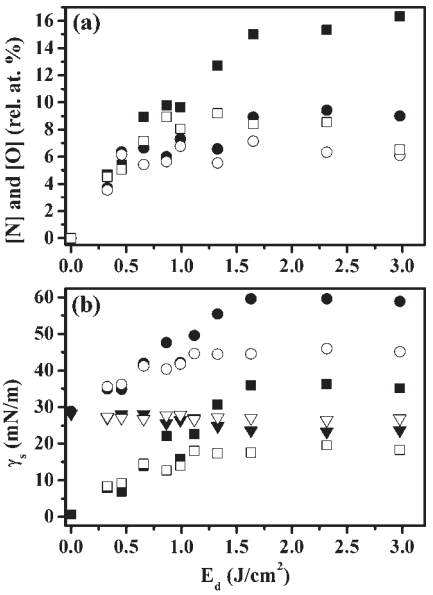


**Figure 5** Effect of water rinsing on $N_2$ APGD treated LDPE, as a function of the energy dose, $E_d$. (a) Surface concentrations of nitrogen, [N], (■), and oxygen, [O] (●). (b) Surface energy, $\gamma_s$, (●), and its polar, $\gamma_s^p$, (■), and dispersive, $\gamma_s^d$, (▼), components. Open symbols pertain to the rinsed samples.

We should emphasize that the presence of LMWOM on the nonrinsed, as-treated surfaces renders the validity of contact angle data or similar measurements highly questionable. Indeed, the thermodynamic interpretation of such experiments assumes that the probe liquids are not contaminated or modified by contact with the surfaces. Furthermore, for the case of samples treated at elevated $E_d$ values, it is probable that some fraction of the LMWOM sublimates in the ultrahigh vacuum of the XPS instrument. Therefore, the nominal values of $\gamma_s$ and [O] reported here for nonrinsed samples must be interpreted with caution.

Experimental data similar to those presented in Figure 2, but for the case of $N_2$ APGD treatments of BOPP, are shown in Figure 3(a, b). Here, too, we use the term LMWOM, even though the nitrogen-containing products obviously differ from their air corona-generated counterparts. In other words, we use the term LMWOM to refer to water-soluble degradation products in a very general way.

Comparing Figures 2(b) and 3(b), we note that even after rinsing, $N_2$ APGD treatments can result in significantly higher $\gamma_s$ values ($\sim$ 40 mN/m versus $\sim$ 33 mN/m for air corona). This is substantiated in Figures 2(a) and 3(a) by the fact that the total combined concentrations of heteroatoms ([O] and [N]) on the washed surfaces are higher following the $N_2$ APGD modifications (8% versus 4% for corona). The presence of bound oxygen after $N_2$ APGD treatments may result from a residual concentration of $O_2$ and water in the discharge gas, or from post treatment reactions of long-lived free radicals on the polymer surface, which occur when the sample is reexposed to ambient atmosphere.[20]

From Figure 3, we note that the threshold for LMWOM production appears at a much higher $E_d$ value, $\sim$ 0.3 J/cm$^2$, compared with 0.01 J/cm$^2$ for air corona. This striking difference may probably be attributed to several factors: first, the concentration of reactive species in an air DBD is much higher than in nitrogen: the free radicals at the polymer surface can readily react with all oxygen-based gaseous species ($O_2$, O, OH, etc.), but not with ground-state molecular nitrogen, which is quite inert. On the other hand, in a pure nitrogen DBD, the dominant reactive species are atomic nitrogen radicals and vibrationally excited $N_2$*, which both require relatively high energy to create.[19] This also explains the slower rise in surface functionalization with increasing $E_d$ in Figure 3. Second, in the

**TABLE I**
**LMWOM Energy Dose Threshold, $E_d$*, and Maximum Surface Energy after Rinsing, $\gamma_{s\ max}$, for both Polymers and both Treatment Types**

| Polymer | Treatment type | $\gamma_{s\ max}$ (mN/m) | $E_d$* (J/cm$^2$) |
|---|---|---|---|
| BOPP | Air corona | 33 | 0.01 |
| | $N_2$ APGD | 40 | 0.3 |
| LDPE | Air corona | 40 | 0.015 |
| | $N_2$ APGD | 45 | 0.5 |

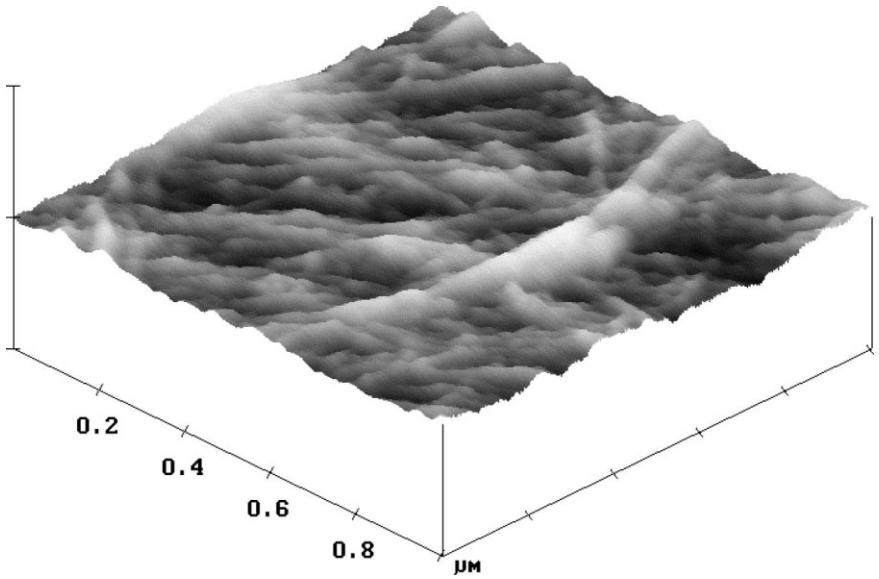


**Figure 6** AFM image of the untreated virgin BOPP surface. Vertical scale: 100 nm.

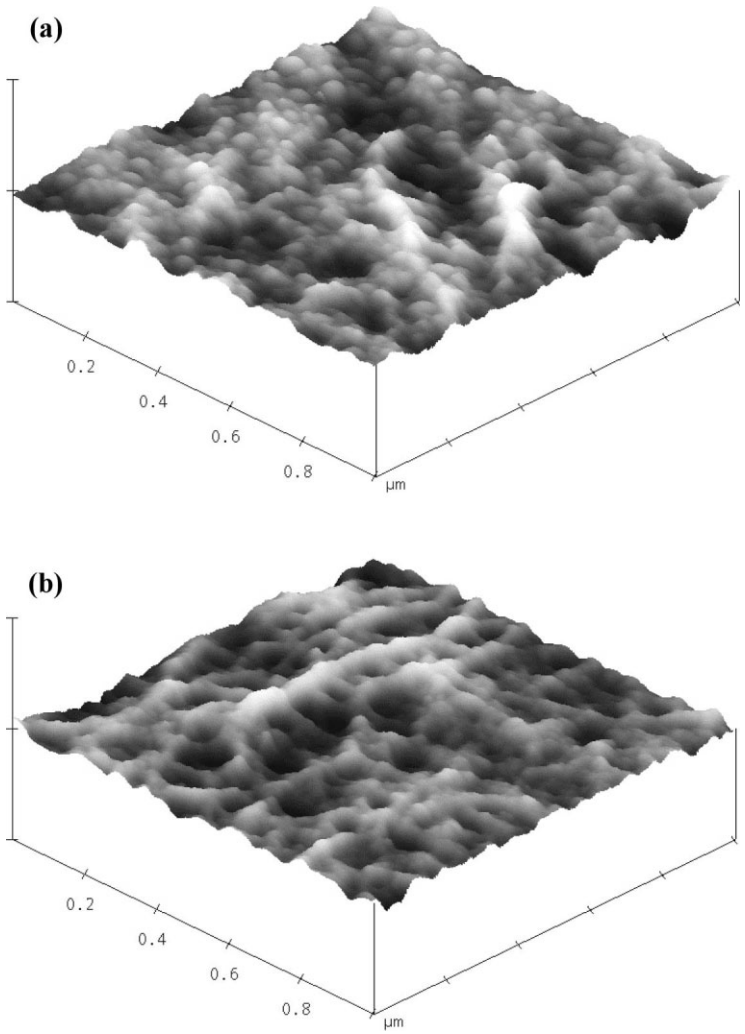


**Figure 7** AFM images of an air corona treated ($E_d$ = 0.04 J/cm$^2$) BOPP sample showing the (a) as-treated and (b) rinsed surfaces. Vertical scale: 100 nm.

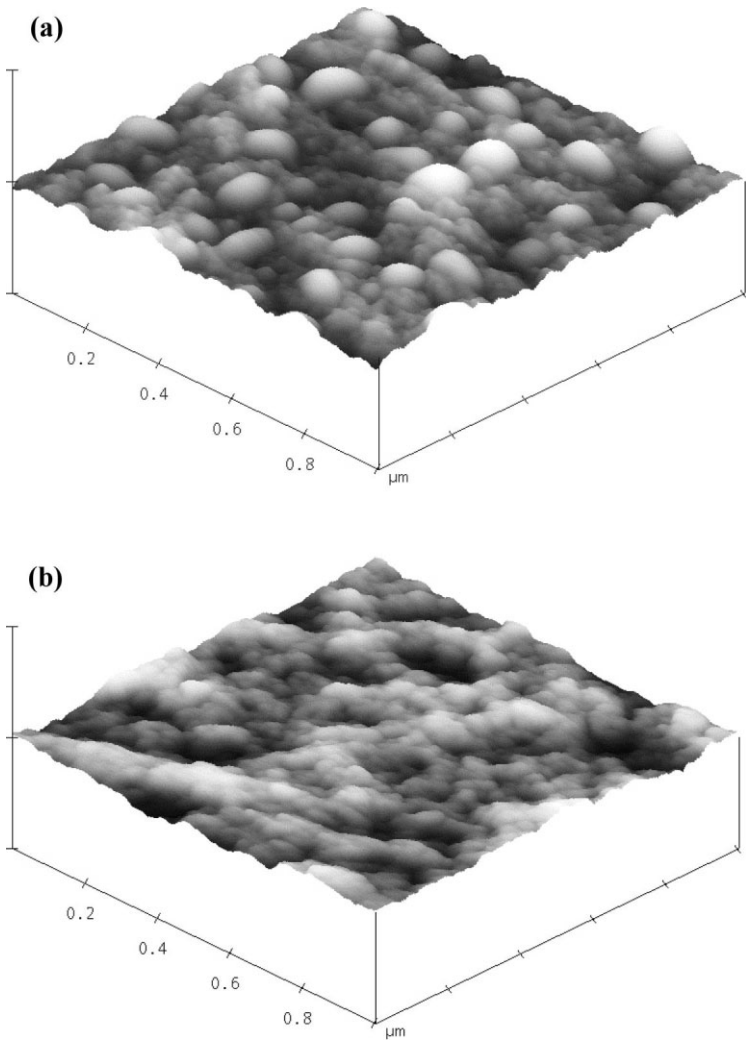


**Figure 8** AFM images of an air corona treated ($E_d$ = 0.4 J/cm$^2$) BOPP sample showing the (a) as-treated and (b) rinsed surfaces. Vertical scale: 100 nm.

case of air DBD, the energy is dissipated highly locally in the filamentary microdischarge channels (diameter $\sim$ 100 $\mu$m), contrary to the uniformly distributed dissipation of energy over the whole area of the treated material in the case of $N_2$ APGD. Finally, and most importantly, the chemical mechanisms associated with the incorporation of N and O at the surface of polypropylene are different, whereby the former reactions induce less chain scissions. In the case of the oxidation of polyolefins, the main-chain C—C bond cleavages occur primarily through $\beta$-scission reactions.[29,30] These follow the formation of alkoxy radicals from the reaction of near-surface alkyl radicals with atomic oxygen, and they lead to the formation of carbonyl groups:

$$—CH_2—HC^{\bullet}—CH_2— \rightarrow —CH_2—HCO^{\bullet}—CH_2— \rightarrow —HC{=}O + {}^{\bullet}CH_2— \quad (2)$$

On the other hand, our earlier studies have shown that amino groups appear to be the main new species introduced at the surface of BOPP during $N_2$ APGD treatment.[20] It therefore seems highly unlikely that appreciable $\beta$-scission reactions could be involved in that case.

From all of the above considerations, it appears that $N_2$ APGD treatments result in much less degradation of the BOPP surface than exposure to air corona. This, in turn, results in the higher degree of surface functionalization, that is, the higher $\gamma_s$, [N], and [O] values observed in Figure 3. The lower amount of LMWOM is probably mostly due to the different chemistry, as also suggested by results of Massines et al.[19] Although these authors did not report on LMWOM formation, they showed that adding traces of $O_2$ to the $N_2$ APGD feed gas (below the impurity level leading to a filamentary discharge regime) greatly reduced the attainable functionalization level of BOPP.

The same comparative studies as those portrayed in Figures 2 and 3 for BOPP have also been carried out for LDPE. The results are presented in Figures 4 and 5 for air corona and for $N_2$ APGD treatments, respectively. Clearly, both treatment types result in some-

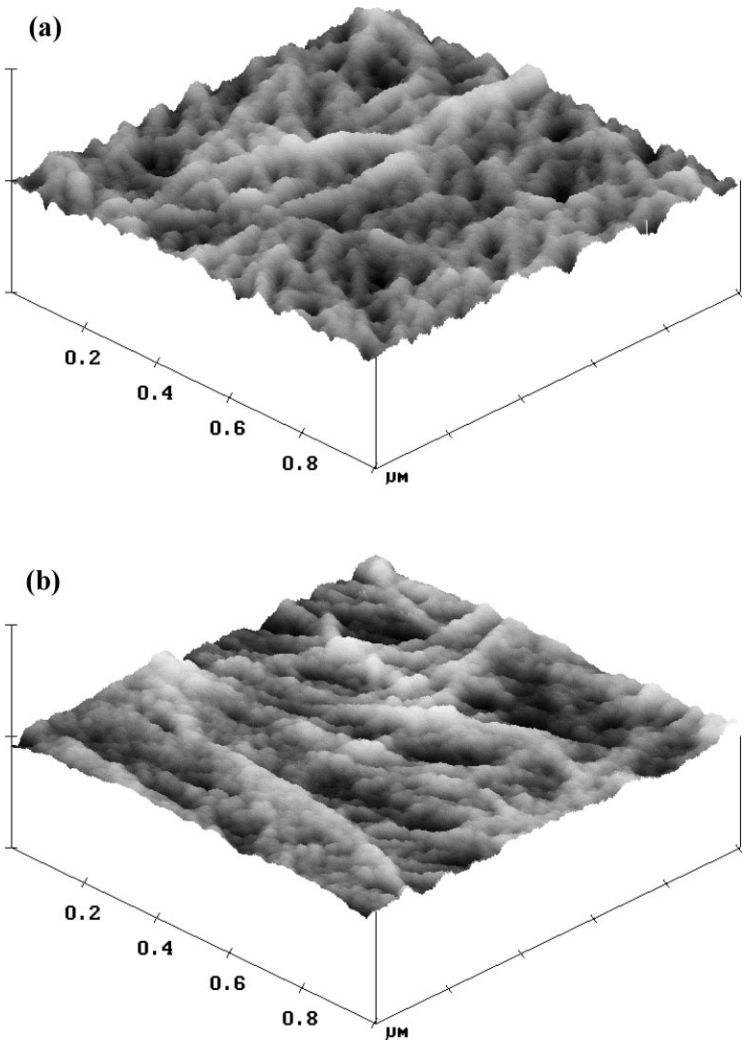


**Figure 9** AFM images of a $N_2$ APGD treated ($E_d$ = 1.1 J/cm$^2$) BOPP sample showing the (a) as-treated and (b) rinsed surfaces. Vertical scale: 100 nm.

what higher $\gamma_s$ values for LDPE than for BOPP. Also, comparing the $E_d$ threshold values for LMWOM generation (Table I), LDPE clearly appears to be less prone to degradation than BOPP, in agreement with data from the literature.[3,7] As in the case of BOPP, $N_2$ APGD treatment of LDPE results in less surface degradation and leads to higher $\gamma_s$ values than air corona. The main results obtained for the two treatment types of both polymers are succinctly summarized in Table I. We now turn to our AFM study of the morphologies of modified BOPP and LDPE films.

### LMWOM production: Surface morphology observations

Many authors have observed the agglomeration of LMWOM on treated polymer surfaces, using AFM[4,10,15,30–33] and scanning electron microscopy (SEM).[3,12] Possibly by the combined effects of surface tension and atmospheric moisture adsorption, the small, mobile LMWOM oligomers generally form nodules or mounds on the treated polymer surfaces. We have investigated this for both of our treatment types and both polymers, before and after rinsing with water. As previously, we begin with the case of BOPP.

A typical AFM image of the untreated, virgin BOPP surface is presented in Figure 6, which clearly shows a fine fibrillar structure that stems from the biaxial orientation of the film.[10] From Figure 7(a), we note that even at a low energy density ($E_d$ = 0.04 J/cm$^2$) air corona treatment produced a significant quantity of LMWOM, visible in the form of many small nodules or droplets. These have diameters of $\sim$ 10 nm, and they disappear after rinsing the film with water. The initial fibrillar structure is still observable on the rinsed surface [Fig. 7(b)], but it is seen to have been altered by the treatment.

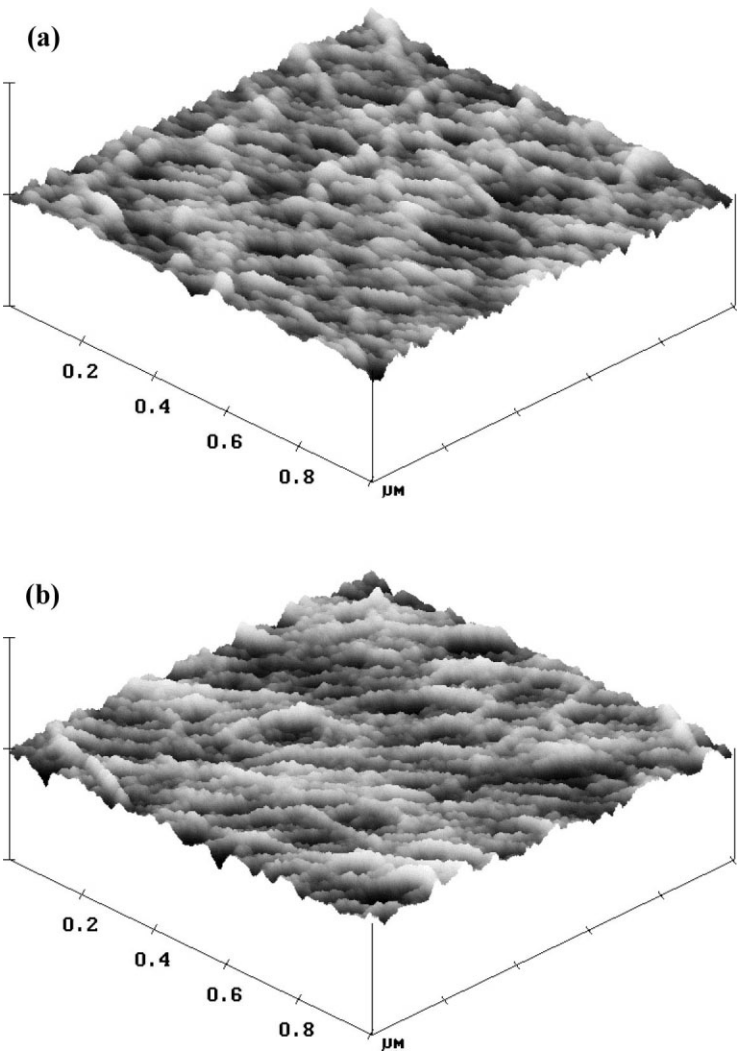


**Figure 10** AFM images of a $N_2$ APGD treated ($E_d$ = 1.7 J/cm$^2$) BOPP sample showing the (a) as-treated and (b) rinsed surfaces. Vertical scale: 100 nm.

After air corona exposures at higher $E_d$ values, the production and agglomeration of LMWOM at the BOPP surface becomes even more evident. For $E_d$ = 0.4 J/cm$^2$ [Fig. 8(a)], the globular features had an average diameter of ~ 50 nm. After rinsing [Fig. 8(b)], the initial topography (Fig. 6) had been greatly modified, indicating substantial etching of the surface during corona treatment. Generally, these observations agree quite well with the contact angle and XPS data presented earlier, for example, that the amount of LMWOM generated increases with rising $E_d$, starting at $E_d$ ~ 0.01 J/cm$^2$.

In the case of $N_2$ APGD treatments (Figs. 9 and 10), the agglomeration of LMWOM appears to be much less important. For $E_d$ = 1.1 J/cm$^2$ [Fig. 9(a)], the fibrils seem to be only slightly altered, being covered with very tiny nodules. Moreover, the topographies of the rinsed [Fig. 9(b)] and as-treated [Fig. 9(a)] surfaces are not very dissimilar, surprising in view of the fact that the energy dose used here substantially exceeded the threshold value for LMWOM production ($E_d$ ~ 0.3 J/cm$^2$). It therefore would appear that the degradation products resulting from $N_2$ APGD treatments agglomerate less and remain more uniformly distributed on the fibrillar surface.

How can these observations be explained? Some plausible answers may be the following: If we assimilate LMWOM to a viscous liquid, it first appears that degradation is more important in the case of air corona, which leads to a LMWOM of smaller average molecular mass, lower viscosity, and greater mobility. Given that $\gamma_s$ of the underlying (modified) polymer surface is lower than in the case of $N_2$ APGD, the LMWOM readily dewets the surface; that is, it is energetically favorable for it to bead up and agglomerate in the form of the observed tiny droplets or nodules. On the other hand, the chemically quite distinct LMWOM generated by $N_2$ APGD appears to have a higher molecular weight and viscosity. Furthermore, because the underlying modified polymer has a sig-

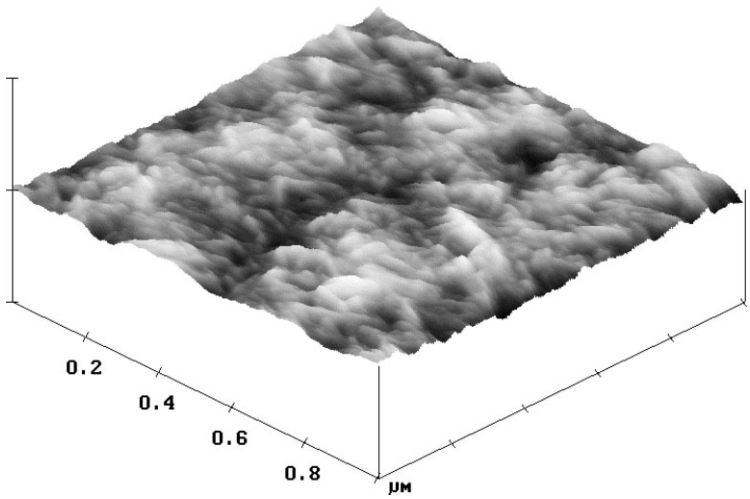


**Figure 11** AFM image of the untreated virgin LDPE surface. Vertical scale: 100 nm.

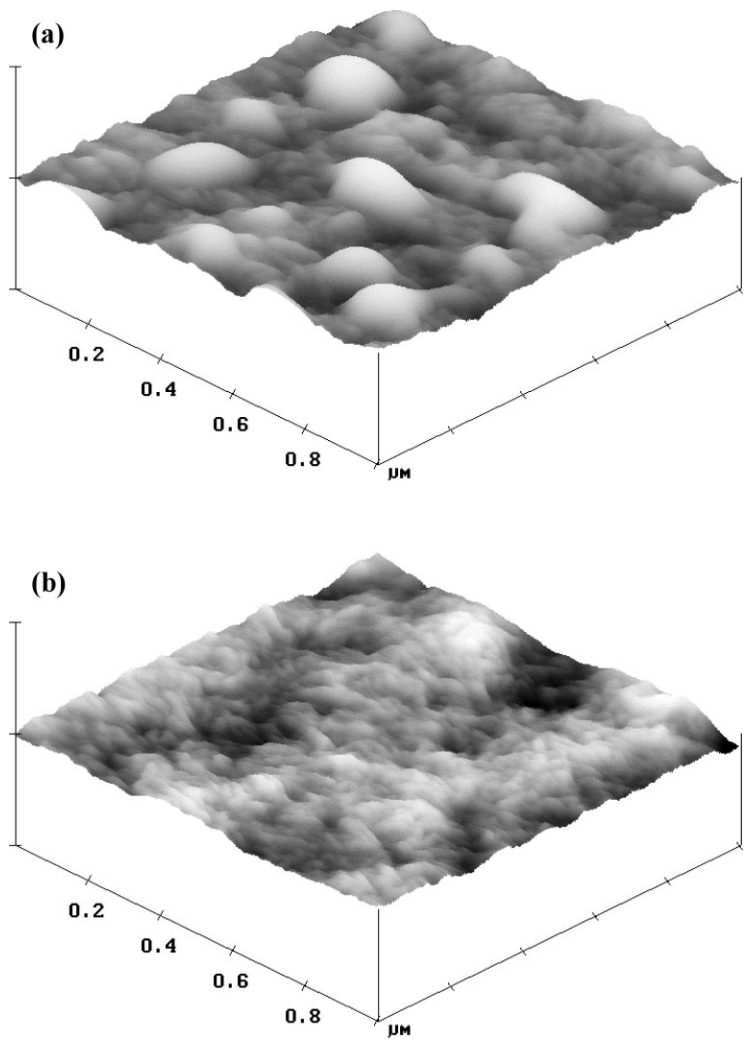


**Figure 12** AFM images of an air corona treated ($E_d$ = 0.7 J/cm$^2$) LDPE sample showing the (a) as-treated and (b) rinsed surfaces. Vertical scale: 100 nm.

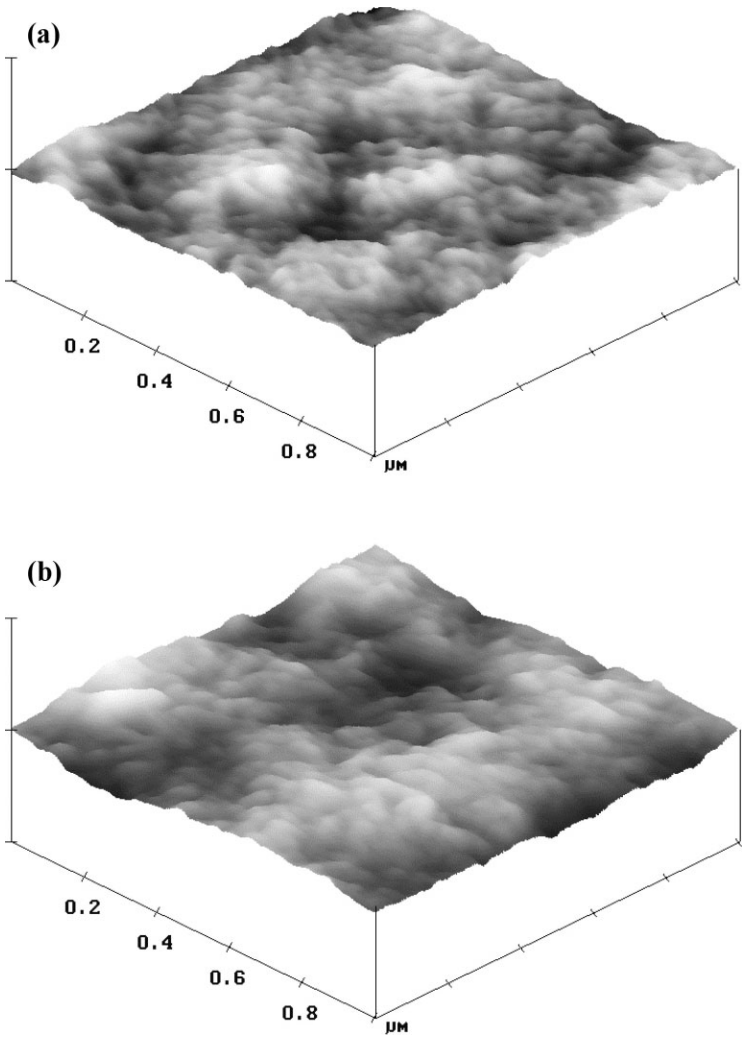


**Figure 13** AFM images of a $N_2$ APGD treated ($E_d$ = 2.3 J/cm$^2$) LDPE sample showing the (a) as-treated and (b) rinsed surfaces. Vertical scale: 100 nm.

nificantly higher $\gamma_s$ value, the tendency to dewet is much reduced, hence, the observed lesser propensity to form droplets.

This proposed scenario seems to be confirmed in Figure 10. Here, AFM images of BOPP treated by higher energy $N_2$ APGD ($E_d$ = 1.7 J/cm$^2$) are presented, where a substantial amount of LMWOM is likely to have been produced (see Fig. 3). Nevertheless, the fibrils appear to be largely intact and mostly very small globules appear on the surface. The difference between the rinsed and as-treated topographies is minimal, although some larger nodules may appear to have been removed by rinsing.

Similar conclusions may also be drawn in the case of LDPE. An AFM image of the untreated, virgin polymer is shown in Figure 11, a surface that appears smoother and unlike the fibrillar structure of BOPP. After air corona ($E_d$ = 0.7 J/cm$^2$), the formation of large globules of LMWOM is clearly observed [Fig. 12(a)], which are completely removed by rinsing with water, as shown in Figure 12(b). Another LDPE sample was modified by $N_2$ APGD at high energy density ($E_d$ = 2.3 J/cm$^2$), well above the LMWOM threshold of $E_d$ = 0.5 J/cm$^2$. Figure 13(a,b), AFM images of the as-treated and rinsed surfaces, respectively, are difficult to distinguish from one another because no LMWOM agglomeration is observable, rather like in the case of BOPP.

### Hydrophobic recovery

The $\gamma_s$ values of selected treated samples have been monitored during storage periods exceeding 100 days for BOPP, and up to 200 days for LDPE; results are shown in Figures 14 and 15, respectively, for different $E_d$ values (nonrinsed films only). For reasons given earlier, $\gamma_s$ values of surfaces with much LMWOM must be considered with caution; nevertheless, we believe that they can provide some useful semiquantitative information about wettability and that they

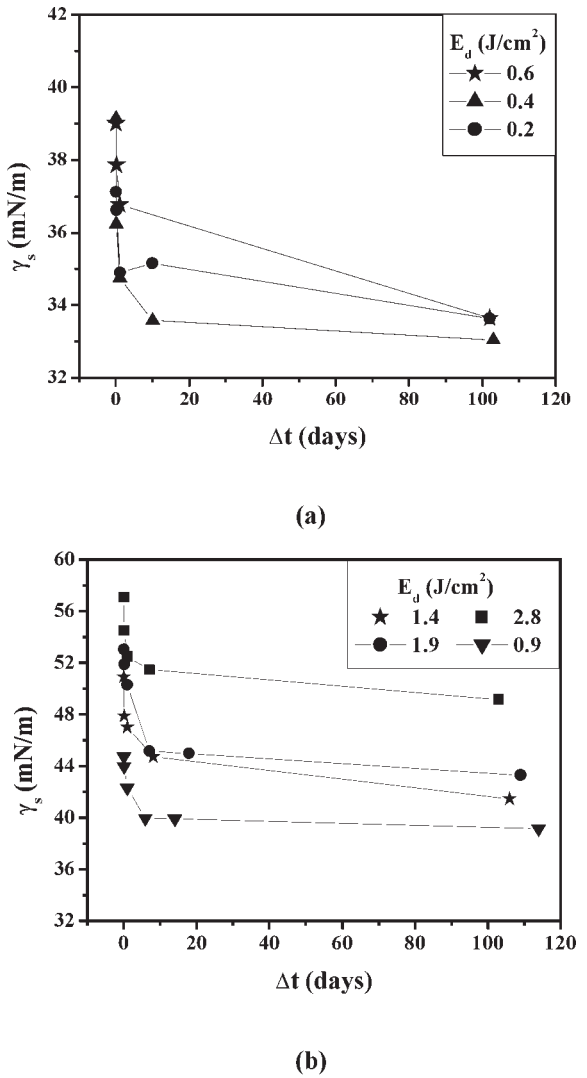


**Figure 14** Surface energy, $\gamma_s$, as a function of the storage time after treatment, $\Delta t$, for several BOPP samples treated by (a) air corona and (b) $N_2$ APGD, with different $E_d$ values.

can be used for comparative purposes. Both figures show that in all cases $\gamma_s$ decreased rapidly during the first week after treatment. For the case of $N_2$ APGD treatments [Figs. 14(b) and 15(b)], $\gamma_s$ is then seen to have stabilized at quite high values (often above 40 mN/m), decreasing at most by 2 or 3 mN/m after several months. For the samples modified by air corona [Figs. 14(a) and 15(a)], $\gamma_s$ also remained relatively stable after its initial decrease. However, its values were then much lower than for the $N_2$ APGD treated samples. After about 3 months of aging, BOPP surfaces treated in air were characterized by $\gamma_s < 34$ mN/m, regardless of the initial energy dose used. In the case of LDPE [Fig. 15(a)], $\gamma_s$ was invariably inferior to 37 mN/m after 200 days of aging, for all $E_d$ values investigated.

We can therefore conclude that, compared to customary air corona treatments, the modification of polyolefins by $N_2$ APGD leads to significantly higher wettability, even after long aging periods. This may represent a major advantage in applications requiring this characteristic (printing with water-based inks, for instance), whereas $\gamma_s$ values of PP and PE modified by air corona are usually insufficient after lengthy storage following treatment.[34]

Several mechanisms have been proposed to explain the hydrophobic recovery of plasma-treated polymers.[27] These include the reorientation of polymer chains so as to bury covalently bonded polar functional groups, the adsorption of adventitious contaminants, the migration of additives toward the surface, and the diffusion of LMWOM towards the bulk of the material. In our case, the exudation of additives can be excluded, because the films investigated contain either no additives or only traces. Also, XPS analyses did not

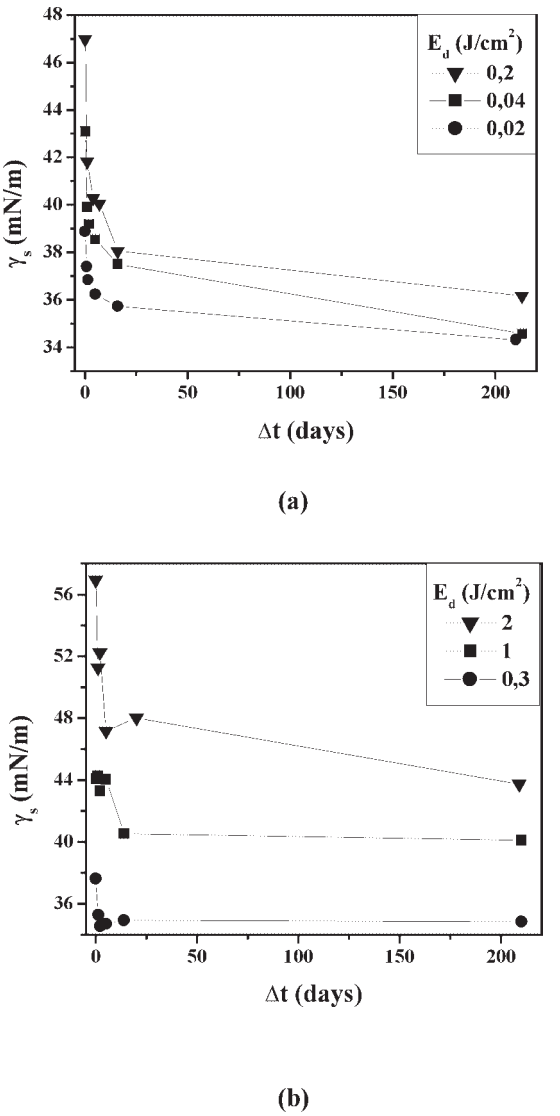


**Figure 15** Surface energy, $\gamma_s$, as a function of the storage time after treatment, $\Delta t$, for several LDPE samples treated by (a) air corona and (b) $N_2$ APGD, with different $E_d$ values.

manifest any significant variations of the surface compositions after storage, indicating that sublimation or inward diffusion of LMWOM did not appear to play an important role. Finally, time of flight secondary ion mass spectrometry (ToF-SIMS) investigations on our samples did not reveal any build-up of atmospheric contaminants on the treated surfaces. It would thus appear that hydrophobic recovery observed here was primarily due to reorientation of polar moieties towards the subsurface. This conclusion, although preliminary, agrees with the findings of Strobel et al.[17] and Occhiello et al.,[35] respectively, who studied the aging of air corona treated and low pressure oxygen plasma treated PP surfaces.

## CONCLUSION

Surface energy, XPS, and AFM data presented in this work allow us to conclude that $N_2$ APGD treatments of BOPP and LDPE surfaces result in significantly less degradation and LWMOM production than conventional air corona. Consequently, the polyolefins can impart higher $\gamma_s$ values and higher degrees of chemical functionalization with $N_2$ APGD. The observed differences derive from the fact that air corona and $N_2$ APGD are governed by very different physics and chemistries when interacting with polymer surfaces.

Even though both methods are subject to hydrophobic recovery, $\gamma_s$ stabilizes quite rapidly at relatively high values after $N_2$ APGD, contrary to the case of air corona treatments. The observed aging appears to result from thermodynamically driven reorientations of polymer chains, which reduce $\gamma_s$ by burying polar groups in the subsurface region.

This work constitutes part of the scientific program of the NSERC Industrial Research Chair on Plasma Processing of Materials. The authors thank Dr. Mark Strobel (3M Co.) and Gary Jerdee (Chevron Phillips Chemical Co.) for kindly providing the BOPP and the LDPE materials, respectively.

## References

1. Briggs, D. in Surface Analysis and Pretreatment of Plastics and Metals; Brewis, D. B., Ed.; Macmillan: New York, 1982; pp. 199–226.
2. Mittal, K. L.; Pizzi, A., Eds. Adhesion Promotion Techniques; Marcel Dekker: New York, 1999.
3. Strobel, M.; Dunatov, C.; Strobel, J. M.; Lyons, C. S.; Perron, S. J.; Morgen, M. C. J Adhesion Sci Technol 1989, 3, 321.
4. O'Hare, L.-A.; Leadley, S.; Parbhoo, B. Surf Interface Anal 2002, 33, 335.
5. Kogelschatz, U. Plasma Chem and Plasma Processing 2003, 23, 1.
6. Wagner, H.-E.; Brandenburg, R.; Kozlov, K. V.; Sonnenfeld, A.; Michel, P.; Behnke, J. F. Vacuum 2003, 71, 417.
7. Gerenser, L. J.; Elman, J. F.; Mason, M. G.; Pochan, J. M. Polymer 1985, 26, 1162.
8. Pochan, J. M.; Gerenser, L. J.; Elman, J. F. Polymer 1986, 27, 1058.
9. Carley, J. F.; Kitze, P. T. Polym Eng Sci 1980, 20, 330.
10. Boyd, R. D.; Kenwright, A. M.; Badyal, J. P. S.; Briggs, D. Macromolecules 1997, 30, 5429.
11. Briggs, D.; Kendall, C. R.; Blythe, A. R.; Wootton, A. B. Polymer 1983, 24, 47.
12. Kim, C. Y.; Goring, D. A. I. J Appl Polym Sci 1971, 15, 1357.
13. Briggs, D.; Rance, D. G.; Kendall, C. R.; Blythe, A. R. Polymer 1980, 21, 895.
14. Foulon-Belkacemi, N.; Goldman, M.; Goldman, A. 11th Int Symp Plasma Chemistry (ISPC 11); Loughborough, 1993; p. 1210.
15. Overney, R. M.; Lüthi, R.; Haefke, H.; Frommer, J.; Meyer, E.; Güntherodt, H.-J.; Hild, S.; Fuhrmann, J. Appl Surf Sci 1993, 64, 197.
16. Strobel, M.; Lyons, C. S. J Adhesion Sci Technol 2003, 17, 15.
17. Strobel, J. M.; Strobel, M.; Lyons, C. S.; Dunatov, C.; Perron, S. J. J Adhesion Sci Technol 1991, 5, 119.
18. Massines, F.; Messaoudi, R.; Mayoux, C. Plasmas Polym 1998, 3, 43.
19. Massines, F.; Gouda, G.; Gherardi, N.; Duran, M.; Croquesel, E. Plasmas Polym 2001, 6, 105.
20. Guimond, S.; Radu, I.; Czeremuszkin, G.; Carlsson, D. J.; Wertheimer, M. R. Plasmas Polym 2002, 7, 71.
21. Yializis, A.; Pirzada, S. A.; Decker, W. in Polymer Surface Modification: Relevance to Adhesion; Mittal, K. L., Ed.; VSP, Zeist (NL); 2000; pp. 65–76.
22. Kanazawa, S.; Kogoma, M.; Moriwaki, T.; Okazaki, S. J Phys D: Appl Phys 1988, 21, 838.
23. Massines, F.; Rabehi, A.; Decomps, P.; Gadri, R. B.; Ségur, P.; Mayoux, C. J Appl Phys 1998, 83, 2950.
24. Massines, F.; Gouda, G. J Phys D: Appl Phys 1998, 31, 3411.
25. Miralaï, S. F.; Monette, E.; Bartnikas, R.; Czeremuszkin, G.; Latrèche, M.; Wertheimer, M. R. Plasmas Polym 2000, 5, 63.
26. Gherardi, N.; Massines, F. IEEE Trans Plasma Sci 2001, 29, 536.
27. Garbassi, F.; Morra, M.; Occhiello, E. Polymer Surfaces, From Physics to Technology, 2nd ed.; Wiley: Chichester, 1998.
28. Kaelble, D. H. Physical Chemistry of Adhesion; Wiley: New York, 1971.
29. Carlsson, D. J.; Wiles, D. M. J Macromol Sci, Rev Macromol Chem 1976, C14, 65.
30. Strobel, M.; Sullivan, N.; Branch, M. C.; Jones, V.; Park, J.; Ulsh, M.; Strobel, J. M.; Lyons, C. S. J Adhesion Sci Technol 2001, 15, 1.
31. Hill, J. M.; Karbashewski, E.; Lin, A.; Strobel, M.; Walzak, M. J. J Adhesion Sci Technol 1995, 9, 1575.
32. Ton-That, C.; Teare, D. O. H.; Campbell, P. A.; Bradley, R. H. Surf Sci 1999, 433, 278.
33. Nie, H.-Y.; Walzak, M. J.; Berno, B.; McIntyre, N. S. Appl Surf Sci 1999, 144, 627.
34. Markgraf, D. A. Coextrusion Conference; Atlanta, GA, 1986; p. 85.
35. Occhiello, E.; Morra, M.; Morini, G.; Garbassi, F.; Humphrey, P. J Appl Polym Sci 1991, 42, 551.